DOI: 10.36253/ijam-2782

Effect of future climate on crop production in Bhutan

Jorge Alvar-Beltrán[a], Gianluca Franceschini[a]

[a]Food and Agriculture Organization (FAO) of the United Nations, Rome (Italy)

Corresponding author: jorge.alvarbeltran@fao.org

Abstract

Understanding the relationship between adverse weather conditions and crop productivity is the backbone of risk assessments on food security. It is paramount in countries like Bhutan, which has a limited number of impact assessment studies in agriculture. The work presented here highlights agricultural production trends under a changing climate and the attribution of yield changes to a specific weather hazard. Thus, the relationship between climate and yields is improved by running the Food and Agriculture Organization (FAO) Python Agroecological Zoning (PyAEZ) model based on state-of-the-art climate projections from the Coordinated Regional Climate Downscaling Experiment (CORDEX-CORE). At the national level, we analyze climate change impacts on yields for ten crops (grain maize, foxtail millet, buckwheat, wheat, wetland rice, common beans, cabbage, white potatoes, carrots, and citrus). The main simulation findings point to higher yield variations, either a gain or a loss, under rainfed conditions as well as for the Representative Concentration Pathway (RCP) 8.5 as opposed to irrigated conditions and RCP 2.6; for example, by +17.4% (white potatoes), +15.3% (wheat), +12.8% (cabbage), -5.8% (citrus), and -6.7% (buckwheat) under RCP 8.5 by 2070-2099. Yield results show the potential of irrigation to modulate adverse weather conditions and to improve crop performance by +43.4% on average for all crops as opposed to rainfed crops which are more exposed to weather hazards (i.e., heat stress and dry spells). This study also sheds light on the most impactful weather perils describing 28% (RCP 2.6) and 33% (RCP 8.5) of the yield variability over time. Thus, the emerging findings support smallholder farmers, decision-makers, and project designers in developing adaptation solutions that minimize the effects of growing adverse weather conditions on crop yields.

Keywords: agricultural meteorology; crop modelling; food security; climate change

1. Introduction

The Kingdom of Bhutan (hereafter Bhutan) is a small landlocked country located on the eastern side of the Himalayas. Historically isolated due to challenging topography, the country's economy is dependent on climate-sensitive sectors such as agriculture, hydropower, and forestry. Subsistence farming is adversely affected by temperature changes and shifting monsoon patterns, while hydropower critically depends on anticipated and stable precipitation patterns, likely to be altered by climate change. According to the National Environmental Commission (NEC, 2023), the country's rich biodiversity and extensive forest cover are already affected by climate change, having cascading consequences for the tourism and services sectors.

This Himalayan country is typically agrarian, with most of the population (56%) relying on agriculture for their livelihoods and accounting for 15% of the country's gross domestic product (ILO, 2019). Smallholder farmers cultivate staple crops (i.e., rice, maize, barley, wheat, and millet) for household consumption. From a socioeconomic standpoint, however, rice, maize, and potato are the three most important crops in Bhutan. Smallholder farmers are particularly vulnerable to changing climatic patterns; even small variations in the departure of the summer monsoon season can have dire consequences on livelihoods. Farmers are increasingly aware of climate change because weather-related impacts represent 10 to 20% of the crop damage (Chhogyel, 2020). Additional studies on farmers' perceptions show that 94% of the farmers perceive a change in local climate, and about 86% are aware of the potential impacts of climate change on their livelihoods (Katwal et al. 2015). For most Bhutanese farmers, climate change means unpredictable weather, less or no rain, and drying of water resources. Farmers also refer to climate change as the arrival of pests and diseases, intensification of rains, less snow cover, and shorter winters.

The limited information on climate extremes in South Asian countries, including Bhutan, is often cited in the literature (Naveendrakumar et al. 2019). Although there are several impact studies assessing the effect of past and future climate on agricultural production in Bhutan, some of the existing literature suggests that weather extremes, including weather-related pests and diseases, are the main drivers of crop production

losses. The latter is particularly important in Bhutan, which, for example, experienced a rice blast epidemic in 1995-96 that resulted in a yield loss of 70 to 90% in high-altitude temperate rice-growing areas. Based on the Ministry of Agriculture and Forests (MoAF, 2011) and NEC (2011) estimates, the grey leaf spot disease severely affected maize production between 2005 and 2007, and by 50% during the 2015 outbreak of maize blight disease; whereas a hailstorm event in 2012 damaged 30 to 40% of the cropland in Punakha (Chhogyel and Kumar, 2018). According to the Department of Agriculture (DoA, 2016), hailstorms and high-intensity rains negatively affected rice-producing areas in 2015 and 2016. Widespread damages to irrigation channels from landslides, triggered by heavy monsoon rains, have also been reported across the country.

Despite increasing efforts to reduce Bhutanese farmers' vulnerability to climate change, the existing policy instruments have not been adequately streamlined into the development plans. There is not yet a clear research and development agenda to mitigate and adapt farming activities to increasing climate adversities (Choden et al. 2020). It is, therefore, paramount to strengthen policy instruments that modulate climate change impacts, enhance smallholder farmers' resilience, and improve crop productivity.

Because of the above reasons, this study applies PyAEZ, which is an assistant tool for countries interested in integrating local-level data into national-level assessments. In the Asia and Pacific region, only a few countries (i.e., Laos, Thailand, and Nepal) have tested PyAEZ (FAO, 2017; Alvar-Beltrán et al. 2023). The study from Alvar-Beltrán et al. (2023), for example, describes PyAEZ simulation constraints (i.e., pests and diseases and CO_2 fertilization effect on crop growth are not considered; reliance on global climate, soil, and land cover datasets are known to be uneven across regions, among others) and various applications for agricultural development planning and for preparing rapid impact assessments in agriculture. Despite these constraints, rapid impact assessments using PyAEZ are necessary for timely decision-making, accelerated response to emergencies, policy formulation, monitoring and evaluation, and risk management. They are indeed particularly important in countries where there is scarce information or obsolete studies. Thus, this work aims to fill the information gap on climate risks in agriculture by strengthening the linkages between weather hazards and impacts on key crops sustaining national food production and the livelihoods of

smallholder farmers across Bhutan. Lastly, it offers a better understanding of the changing climate dynamics and identifies weather perils likely to be harmful to national agricultural production.

2. Materials and Methods

2.1. Area of study

According to Köppen's climatic classification, Bhutan is characterized by a humid sub-tropical climate and a sub-tropical highland oceanic climate (Cwb) in the low-lying areas (< 800 m.a.s.l.), mid-hills (800-1800 m.a.s.l.), and high-hills (1800-3000 m.a.s.l.), respectively (Beck et al. 2005). A temperate continental (Dwb), cool continental (Dwc), and tundra climate (ET) progressively appear towards the higher altitude areas of the Himalayas. As a result of a mosaic of climates, MoAF has divided the country into six agroecological zones, each with singular climatic conditions (Fig. 1). Four of them (wet sub-tropical, humid sub-tropical, dry sub-tropical, and warm temperate) are agriculturally predominant, while one (cool temperate) is considered an agricultural marginal area, and the remaining one (alpine) livestock predominant.

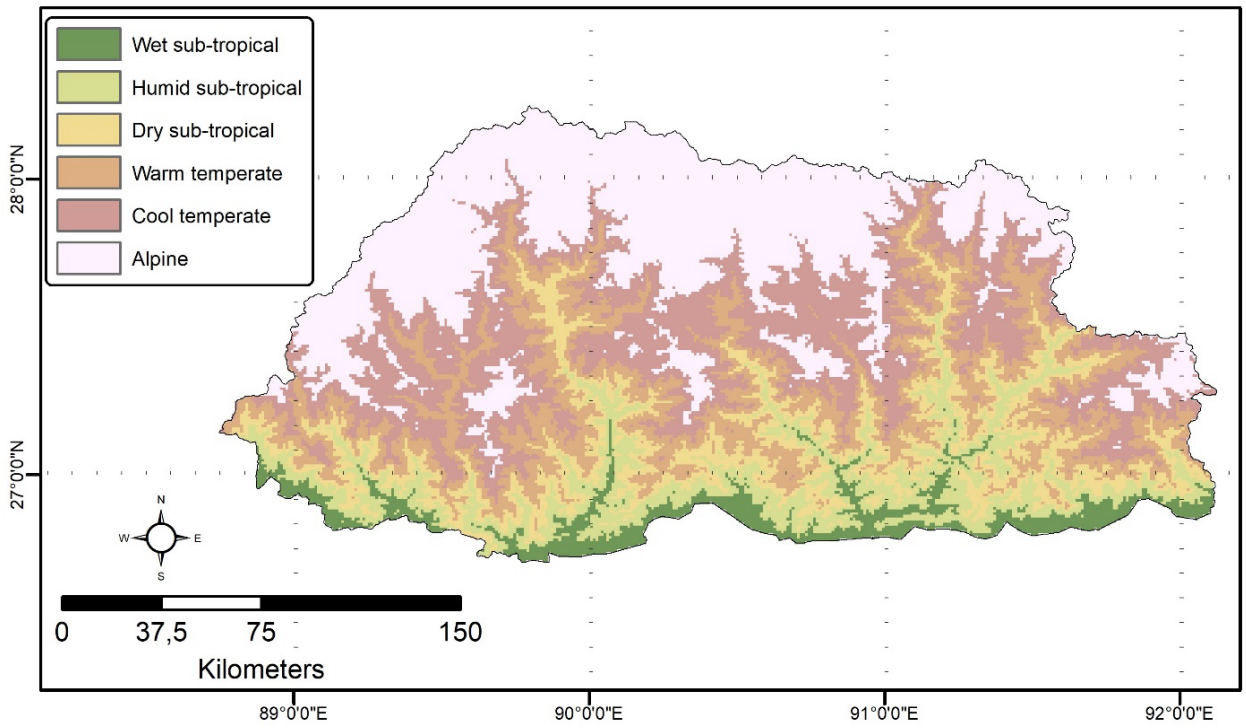

Figure 1. Agroecological zones of Bhutan

2.2. Climate projections

Daily minimum and maximum temperatures, and precipitation data from the Coordinated Regional Climate Downscaling Experiment (CORDEX) - Coordinated Output for Regional Evaluations (CORE) - were used in this study. Briefly, the CORDEX-CORE initiative has created a shared climate modelling framework worldwide (Giorgi et al. 2021) by providing homogeneous regional climate projections for most inhabited land regions using nine CORDEX domains at 0.22º spatial resolution (25 km). Three Global Climate Models (GCMs) for high (HadGEM2-ES), medium (MPI-ESM), and low (NorESM) equilibrium climate sensitivities, representing the full ensemble of the Coupled Model Intercomparison Project (CMIP5), were dynamically downscaled using one Regional Climate Model (RCM), namely REMO, under two Representative Concentration Pathways (RCP), RCP 2.6 and RCP 8.5 (Coppola et al. 2021; Teichmann et al. 2021). For the 1981-2010 historical period, we used the W5E5 merged dataset, which combined the WFDE5 dataset over land with the ERA5 dataset over the ocean (Cucchi et al. 2020). W5E5 is commonly used in impact assessment studies and has been adopted by the Inter-Sectoral Impact Model Intercomparison Project (ISIMIP) as the official product for the bias correction of atmospheric models. Thus, the CORDEX-CORE simulations were bias-corrected using the W5E5 reanalysis dataset for the 1980-2005 period, time slice where both datasets overlap.

2.3. Agroecological zoning (PyAEZ)

Yields were estimated based on an eco-physiological model developed by FAO (Kassam et al. 1991; Kassam, 1977). We adopted the simplified version of AEZ, implemented in Python (PyAEZ), and publicly available through a GitHub repository (https://github.com/gicait/PyAEZ). Geo-referenced global climate (see section 2.2), soil (from the Harmonized World Soil Database at 0-30 and 30-100 cm soil depth), land cover (from the Global Land Cover-SHARE), elevation, and terrain slope data (from the Shuttle Radar Topography Mission) were combined into a land resources database, which was then assembled into global grids at a resolution of 30 arc-seconds (about 0.9 by 0.9 km at the equator) (Fischer et al. 2021; Latham et al. 2014; Nachtergaele et al. 2012). Constraint-free crop biomass was accumulated during the growing season, mainly driven by incoming solar radiation, temperature, and crop-specific characteristics (i.e., growing length, maximum photosynthetic rate, leaf area index (LAI) at full development, harvest index, and crop's sensitivity to heat provision). To maximize yields, the start of the growing season was automatically determined by PyAEZ. Simulations were run on an annual basis independently for rainfed

and irrigated conditions for all ten crops (buckwheat, foxtail millet, grain maize, wetland rice, wheat (subtropical cultivar), common bean, cabbage, white potatoes, carrots, and citrus) and averaged for the 2010-2039, 2040-2069, and 2070-2099 periods. Reference historical yield values (Table 1) were used to bias-correct future crop simulations. Most of the crop parameters (e.g. length of growth cycle, leaf area index, harvest index) were adapted from Fischer et al. (2021), using the cultivar and corresponding crop characteristics that were more common in the country.

The procedure to assess the maximum attainable yield was conducted in PyAEZ by calculating an automatic crop calendar based on the most suitable climatic and perfect management conditions. The simulations were run 365 times per year with a moving window of a day to identify the starting date when the highest final yields were obtained. This meant that the starting growing date changed each year according to the specific annual climatic conditions. While some crops may have multiple growing seasons in a year, only one simulation period was computed per crop, which represented the one providing the highest yield.

The assessment of rainfed yields was done by calculating a daily water balance and applying a yield-reduction factor (associated with yield stress) at each phenological stage. Daily soil moisture balance calculation procedures followed the methodologies outlined by Allen et al. (1998). Briefly, the quantification of a crop-specific water balance determined the crop's actual evapotranspiration (ETa), a measure used for calculating water-constrained crop yields by comparing ETa with a crop's evaporative demand. As a result, the daily reference soil water balance was calculated for each grid cell and actual evapotranspiration was estimated for each crop.

Table 1. Average crop yields (kg/ha) for 2018-2022. Yield values presented in Table 1 were usually lower than those of PyAEZ simulations which considered the maximum attainable yields. Source: FAOSTAT

Crop	Yield (kg/ha)
Maize (corn)	3492.0
Millet	1189.4
Buckwheat	1166.4
Wheat	1310.1
Rice	4240.0
Beans (dry)	1038.4

Cabbage	7146.2
Potatoes	10497.9
Carrots and turnips	10759.2
Citrus (lemons and limes)	3313.7

159

160 2.4. Attributing adverse weather conditions

161 Understanding the impact of adverse weather conditions on simulated crop yields required a dynamic
162 statistical approach to (i) identify adverse weather conditions, (ii) assess the goodness of fit of the statistical
163 model, and (iii) select the best model by dynamically repeating the process. For this reason, we developed
164 a tailored computational and statistical framework (Fig. 2). Briefly, climate models were processed to retain
165 climate information only for the growing period. The selected period was different every year, as PyAEZ
166 adopted a dynamic sowing date approach (see results in supplementary section). Then, adverse weather
167 conditions such as warm days, cold days, dry days, wet days, maximum duration of dry spells, and mean
168 duration of dry spells were computed. Results were spatially averaged and correlated adverse weather
169 conditions were removed. Multiple linear regression was applied to explain the predicted yield. In each
170 case, a dynamic selection of thresholds was used for calculating weather extremes. At the end of the
171 simulation cycle, only the best model (highest R^2) was retained. This R^2 analysis allowed us to discern the
172 most impactful adverse weather conditions on crop yields, describing the percentual change of the output
173 variable (yield) explained by the input variable (adverse weather condition). This approach was then
174 repeated for each crop, year, RCP, and climate model, resulting in around 12,000 simulations.

175

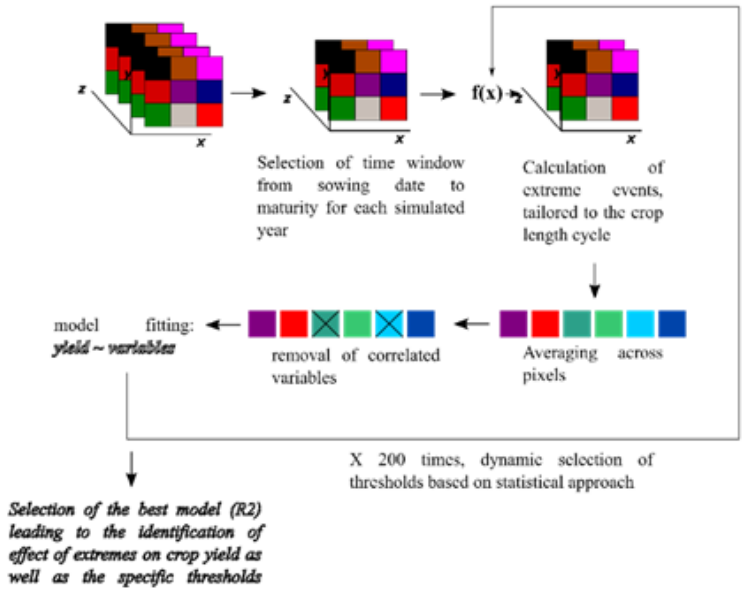

Figure 2. The statistical and computational framework used for the quantification of adverse weather conditions and to assess their impacts on crop yields.

3. Results

3.1. Future climate

For projected precipitation changes, the different climate models and scenarios showed less model agreement. Briefly, total annual precipitation displayed minimal anomalies (positive/negative) in the near (2020-2039) and mid-term (2040-2069) for both RCPs. However, total annual rainfall anomalies were heightened towards the end of the century, with a decline along the low-lying and agricultural predominant areas, particularly under RCP 8.5 (-100 to -200mm/year) and, to a minor extent, under RCP 2.6 (0 to -100mm). Supp. Fig. 1 showed the changes in monthly precipitation across the century and for both RCPs. Projected changes were minimal between November and March and peaked during the summer monsoon season. For example, the wet-subtropical and humid sub-tropical agro-ecological zones were projected to experience a decline in monthly precipitation (June, August and September) ranging from 50 to 150mm/month by 2070-2099 under RCP 8.5. Conversely, cool temperate and alpine climates, corresponding to the non-agricultural predominant areas, were thought to experience an increase during the summer monsoon season of about 50 to 100 mm/month under RCP 8.5 by 2070-2099. Additionally, the pre-monsoon months (April and May) were projected to gain in precipitation, particularly towards the southeast of Bhutan.

196

197 Mean maximum temperature (hereafter Tmax) anomalies were heightened towards the high-altitude
198 areas from January to March (Supp. Fig. 2). Tmax was projected to increase by 1 to 2ºC under RCP 2.6
199 and by 3 to 5ºC under RCP 8.5 by 2070-2099 compared to 1980-2005. Although mean minimum
200 temperature (hereafter Tmin) anomalies displayed a similar spatiotemporal pattern to that of Tmax, the
201 rate of increase was higher across the century. For example, Tmin was projected to increase by 4 to 6ºC,
202 or a staggering 7 to 9ºC over the Himalayas, from January to March under RCP 8.5 by 2070-2099
203 compared to 1980-2005 (Supp. Fig. 3). For both climatic variables (Tmax and Tmin), the spatial changes
204 during the summer monsoon season (from June to September) were softened across Bhutan.

205

206

207 3.2. Crop suitability analysis

208 *3.2.1. Cereal crops*

209 For maize (Fig. 3a) under rainfed conditions, PyAEZ yield simulations showed no significant changes
210 (+0.3%) over time in RCP 2.6 (from 4,064 to 4,077 kg/ha) and a slight loss (-2.1%) in RCP 8.5 (from 4,053
211 to 3,968 kg/ha) between 2010-2039 and 2070-2099. The shortfalls in maize production under RCP 8.5 can
212 also be attributed to a decline in monthly precipitation over the rainy season (June to September),
213 particularly along the mid-hills and low-lying areas of Bhutan (Supp. Fig. 1). Additionally, while all the
214 GCMs agreed on projected yield changes under RCP 2.6, some differences were observed under RCP 8.5,
215 with higher yields simulated in MPI-ESM (4,133 kg/ha) compared to NorESM1-M and HadGEM2-ES
216 (3,920 kg/ha) on average across the century. For irrigated conditions, there were no major yield differences
217 over time. Overall, the average yields simulated across the century under irrigated conditions were 25%
218 higher than those simulated under rainfed conditions for both RCPs and GCMs. Lastly, under perfect
219 management conditions, the most optimal sowing date to attain the highest yields was 117 calendar days
220 for HadGEM2-ES, 114 for NorESM1-M, and 101 for MPI-ESM. However, the trends for the most optimal
221 sowing date showed a delay for NorESM1-M and MPI-ESM, thus, leading to a similar sowing date as that
222 of HadGEM2-ES towards the end of the century (Supp. Fig. 4a).

For foxtail millet (Fig. 3b) under rainfed conditions, yield simulations showed a minimal positive anomaly (+1.4%) over time in RCP 2.6 (from 1,766 to 1,790 kg/ha) and a decreasing trend (-3.4%) in RCP 8.5 (from 1,769 to 1,708 kg/ha) between 2010-2039 and 2070-2099. The monthly precipitation decline over the rainy season largely explained the losses in millet yields, particularly under RCP 8.5 (Supp. Fig. 1). Additionally, remarkable foxtail millet yield anomalies were simulated among different GCMs, especially when comparing HadGEM2-ES and MPI-ESM to NorESM1-M under RCP 2.6. Across the century, the latter two GCMs simulated higher yields (1,804 kg/ha) than NorESM1-M (1,723 kg/ha) under RCP 2.6. On the other hand, for irrigated conditions, PyAEZ simulations did not show major yield differences over time (2,092 kg/ha). However, while HadGEM2-ES and MPI-ESM displayed similar yields (2,077 kg/ha) for both RCPs, NorESM1-M projected a slightly higher yield (2,143 kg/ha) under RCP 8.5. Lastly, large differences were simulated for the most optimal sowing date among GCMs. While NorESM1-M simulated 134 calendar days as the most optimal sowing date, for MPI-ESM it was 112 days. Overall, all models agreed on an earlier sowing date to attain the highest yields (Supp. Fig. 4b).

For buckwheat (Fig. 3c) under rainfed conditions, PyAEZ yield simulations showed no significant anomalies (+0.1%) over time in RCP 2.6 (from 743 to 744 kg/ha) and declining trends (-6.7%) in RCP 8.5 (from 731 to 682 kg/ha) between 2010-2039 and 2070-2099. However, significant yield differences were detected when comparing different GCMs, particularly between HadGEM2-ES and NorESM1-M. In this case, HadGEM2-ES (high sensitivity to GHG emissions) simulated higher yield trends than NorESM1-M (low sensitivity to GHG emissions). Conversely, for irrigated conditions, PyAEZ simulations did not exhibit major differences between RCPs, with an average yield of 1,062 kg/ha across the century. Overall, under irrigated conditions, buckwheat yields were approximately 46% higher compared to those simulated under rainfed conditions. Lastly, under perfect management conditions, all GCMs agreed on a similar sowing date to attain the highest yields, ranging from 152 (HadGEM2-ES) to 138 (MPI-ESM) calendar days (Supp. Fig. 4c). However, different trends on the most optimal sowing date were displayed along the century, with an earlier sowing date of about 10 days for HadGEM2-ES and NorESM1-M and a delay of about 5 days for MPI-ESM.

252 For wheat (Fig. 3d) under rainfed conditions, PyAEZ yield simulations displayed a slight decline (-1.0%)
253 under RCP 2.6 (from 1,245 to 1,232 kg/ha) and a significant yield gain (+15.3%) under RCP 8.5 (from
254 1,227 to 1,415 kg/ha) between 2010-2039 and 2070-2099. The former can be attributed to more optimal
255 temperatures during the winter season and to a slight precipitation increase (e.g. April and May) during the
256 grain filling phase of wheat, particularly under RCP 8.5. Furthermore, under RCP 8.5, all three GCMs
257 agreed on a notable yield increase over time, though with slight differences in the timing of the increase.
258 Similarly, for irrigated conditions, higher wheat yields were simulated under RCP 8.5 (2,142 kg/ha)
259 compared to RCP 2.6 (2,027 kg/ha) by 2070-2099. As with the other crops, interannual yield variability
260 under irrigated conditions was much lower than that simulated under rainfed conditions due to the high
261 variations in soil water balance when fields were not irrigated. Lastly, all three GCMs displayed minor
262 changes in the most suitable sowing date throughout the century. Although the main planting season usually
263 occurs from November to December, PyAEZ simulations pointed to higher yields if sown after 71 calendar
264 days (Supp. Fig. 4d). However, the latter sowing date overlaps with the preparation of land of other crops,
265 such as maize that is usually sown during the spring season.
266
267 For rice (Fig. 3e) under rainfed conditions, PyAEZ simulations showed minimal yield changes (+0.2%)
268 under RCP 2.6 (from 2,052 to 2,057 kg/ha) and a slight decline (-1.6%) under RCP 8.5 (from 2,033 to 2,001
269 kg/ha) between 2010-2039 and 2070-2099. However, under RCP 8.5 for MPI-ESM, simulated yields were
270 estimated to decrease by -7.1% (from 2,076 kg/ha to 1,928 kg/ha) between the 2010-2039 and 2070-2099
271 periods. For irrigated conditions, rice yields remained constant over time, with low interannual yield
272 differences and similar yield values under both RCPs. Generally, large differences of up to 42% (from
273 2,880 kg/ha to 2,027 kg/ha) were observed when comparing the yields simulated under irrigated and rainfed
274 conditions, respectively, across the century for both RCPs. Lastly, all GCMs agreed on a similar sowing
275 date to attain the highest rice yields, ranging from 111 (HadGEM2-ES) to 98 (MPI-ESM) calendar days
276 (Supp. Fig. 4e).
277
278 **a)** **b)**

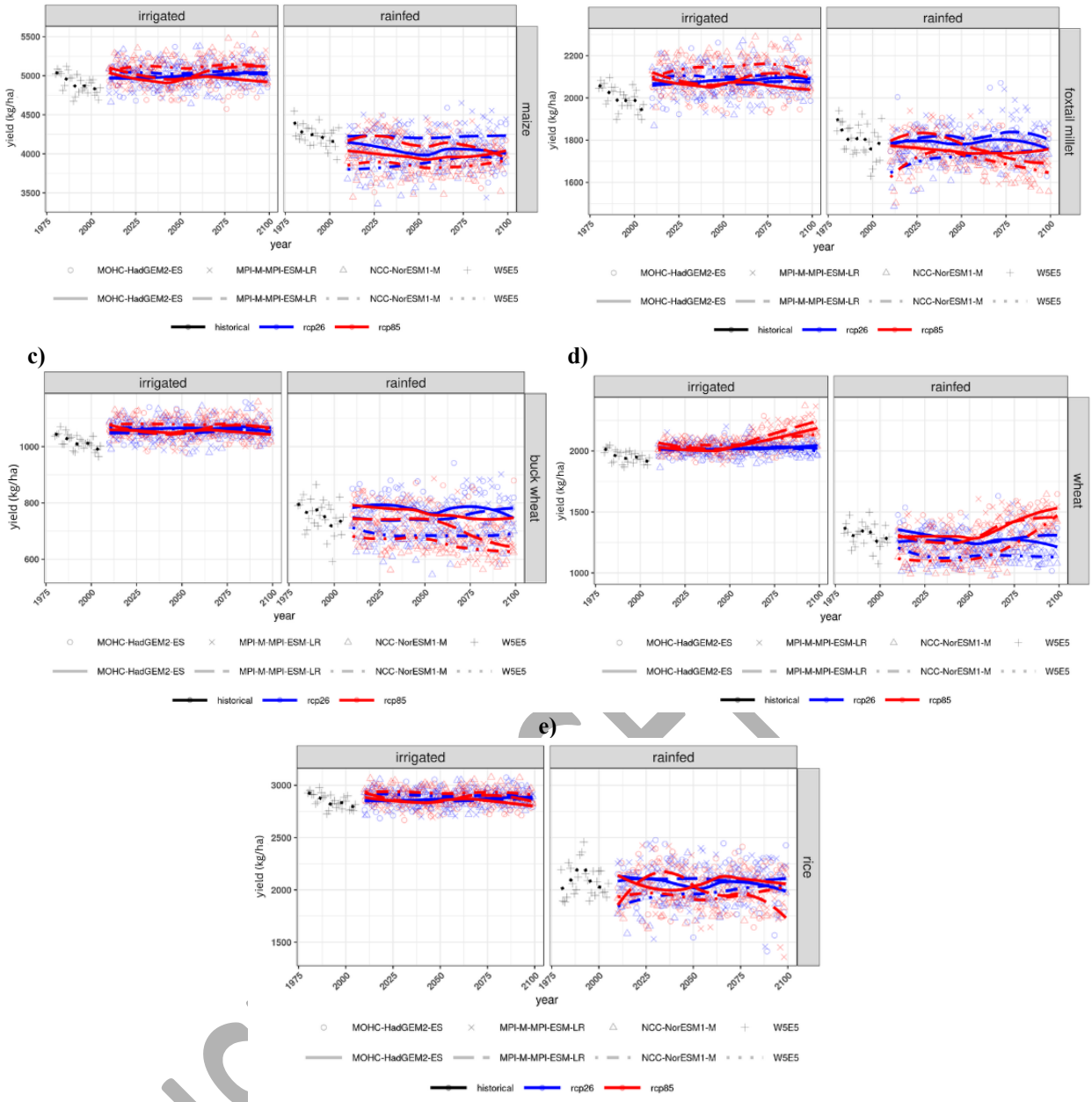

Figure 3. National level yield trends (kg/ha) for **(a)** maize, **(b)** foxtail millet, **(c)** buckwheat, **(d)** wheat, and **(e)** rice under irrigated and rainfed conditions for RCPs 2.6 and 8.5 over the 2010-2099 period. Future yield simulations were based on three GCMs and historical information on the W5E5 dataset.

3.2.2. Legumes, vegetables, and tuber crops

For common beans (Fig. 4a) under rainfed conditions, PyAEZ yield simulations did not display a change (0.0%) in RCP 2.6 and a loss (-4.8%) in RCP 8.5 (from 1,126 to 1,072 kg/ha) between 2010-2039 and 2070-2099. The reported decline under RCP 8.5 was largely due to increasing number of warm days and mean dry spell duration (Fig. 8). Additionally, under RCP 8.5, the negative yield change was expected in the second half of the 21st century. Simulations for common beans showed large inter-annual yield differences

294 between GCMs, particularly under RCP 8.5. Conversely, for irrigated conditions, similar yields (1,410
295 kg/ha) were projected under both RCPs across the century. However, from the mid-century onwards, the
296 yield variability was expected to increase. Overall, the average yield differences across the century between
297 irrigated and rainfed conditions were 26% for both RCPs and all GCMs. Additionally, simulations on the
298 most optimal sowing date to attain the highest yields show large differences across the century (Supp. Fig.
299 4f). On average, HadGEM2-ES simulated the latest sowing date (124 calendar days), while MPI-ESM the
300 earliest sowing date (104 calendar days).
301
302 For cabbage (Fig. 4b) under rainfed conditions, PyAEZ yield simulations did not show anomalies over time
303 (-0.3%) in RCP 2.6 (from 1,893 to 1,888 kg/ha) and a moderate gain (+12.8%) in RCP 8.5 (from 1,865 to
304 2,104 kg/ha) between 2010-2039 and 2070-2099. Under RCP 8.5, the rate of yield enhancement was
305 significant from mid-century until the end of the century. For irrigated conditions, yield trends for cabbage
306 were identical to those simulated for wheat. The average cabbage yield remained constant (2,892 kg/ha)
307 under RCP 2.6, while there was a notable increase under RCP 8.5, especially when comparing 2010-2039
308 (2,907 kg/ha) and 2070-2099 (3,044 kg/ha). Lastly, all GCMs agreed on a similar sowing date to attain the
309 highest cabbage yields, ranging from 72 to 66 calendar days, as well as on a slight delay on the most optimal
310 sowing date across the century (Supp. Fig. 4g).
311
312 For white potatoes (Fig. 4c) under rainfed conditions, PyAEZ yield simulations did not display a major
313 change (-0.6%) over time in RCP 2.6 (from 1,978 to 1,968 kg/ha) and showed a notable increase (+17.4%)
314 in RCP 8.5 (from 1,962 to 2,303 kg/ha) between 2010-2039 and 2070-2099. Under RCP 8.5, all three GCMs
315 showed similar yield trends over time, with a strong increase up until mid-century and a slight to moderate
316 decrease towards the end of the century. Higher inter-annual yield variability was projected under RCP 8.5
317 compared to RCP 2.6. For irrigated conditions, white potato yields were likely to remain constant (+0.8%)
318 under RCP 2.6 and increase (+5.5%) under RCP 8.5 (from 3,525 to 3,719 kg/ha) by 2070-2099 compared
319 to 2010-2039. Overall, significantly higher yields (72%) were expected under irrigated conditions (3,562
320 kg/ha) compared to rainfed conditions (2,067 kg/ha) when averaged across both RCPs and the three GCMs.
321 All three GCMs displayed a similar optimal sowing date (79 calendar days) (Supp. Fig. 4h). The latter
322 matched farmers sowing calendars, as potatoes are traditionally sown in the spring, around March to April.

For carrot (Fig. 4d) under rainfed conditions, PyAEZ yield simulations did not show a change (+0.1%) over time in RCP 2.6 (from 3,344 to 3,346 kg/ha) and a slight loss (-3.9%) under RCP 8.5 (from 3,309 to 3,181 kg/ha) between 2010-2039 and 2070-2099. However, under RCP 8.5, simulations emerging from different GCMs showed divergent behavior, leading to uncertainty over time. While MPI-ESM and NorESM1-M displayed similar yield trends over time (a decrease from 2050 onwards), HadGEM2-ES projected an increase towards the end of the century. On the other hand, under irrigated conditions, carrot yields showed similar performance under both RCPs and across all GCMs when comparing 2010-2039 and 2070-2099. Overall, higher yields (22%) were projected across the century under irrigated conditions (4,018 kg/ha) compared with rainfed conditions (3,288 kg/ha) when averaged across both RCPs and the three GCMs. Regarding the most suitable sowing date, the earliest sowing date to attain the highest yields was simulated by HadGEM2-ES (98 calendar days), while the latest by NorESM1-M (97 calendar days) (Supp. Fig. 4i). All three GCMs agreed on earlier sowing date, 15 to 20 days than baseline values, to attain the highest yields under future climatic conditions.

a) **b)**

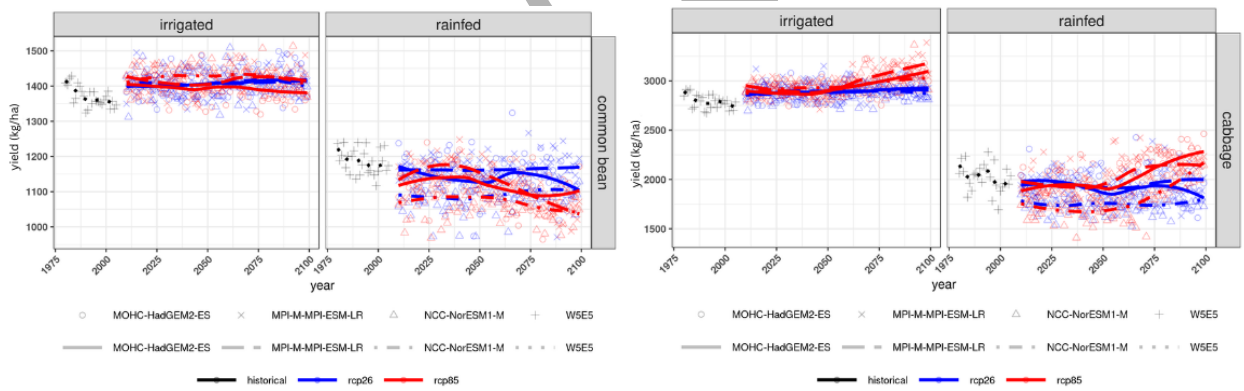

c) **d)**

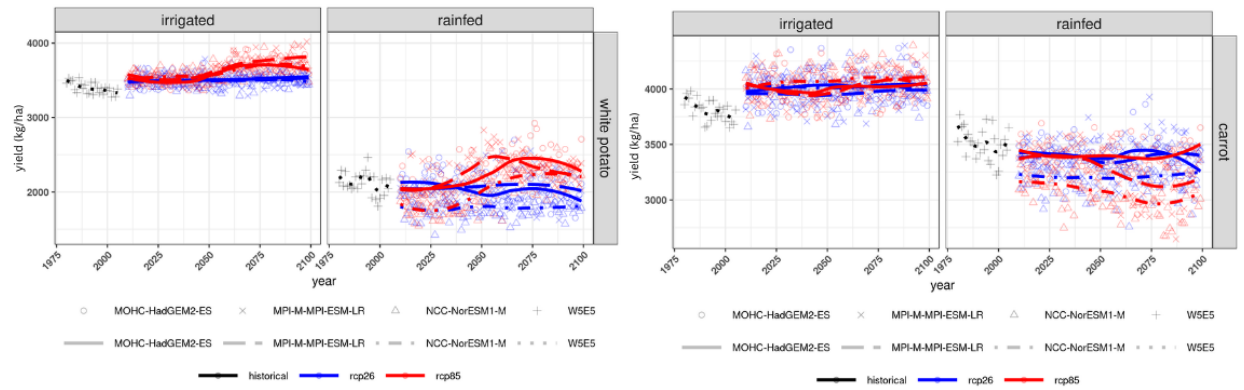

Figure 4. National level yield trends (kg/ha) for **(a)** common beans, **(b)** cabbage, **(c)** white potatoes, and **(d)** carrot under irrigated and rainfed conditions for RCPs 2.6 and 8.5 over the 2010-2099 period. Future yield simulations were based on three GCMs and historical information on the W5E5 dataset.

3.2.3. Tree-crop

For citrus tree (Fig. 5) under rainfed conditions, PyAEZ yield simulations showed a yield loss (-1.9%) in RCP 2.6 (from 2,471 to 2,425 kg/ha) and a moderate decrease (-5.8%) in RCP 8.5 (from 2,404 to 2,264 kg/ha) between 2010-2039 and 2070-2099. The projected decline under RCP 8.5 could be attributed to the compounded effect of several weather perils such as the alternation of warm and cold days as well as dry-spells, particularly during the flowering stage (typically from March to May) (Fig. 8). Although similar yield trends were projected over time for the three GCMs in RCP 8.5, higher average yields were simulated in MPI-ESM and HadGEM2-ES (2,357 kg/ha) compared with NorESM1-M (2,170 kg/ha). For irrigated conditions, citrus yields showed similar performance across both RCPs and all GCMs, though with a slight loss (from 2,917 to 2,901 kg/ha) when comparing 2010-2039 with 2070-2099. Overall, while high inter-annual yield variability was projected under rainfed conditions, low variability was simulated under irrigated conditions due to minimal changes in soil water balance.

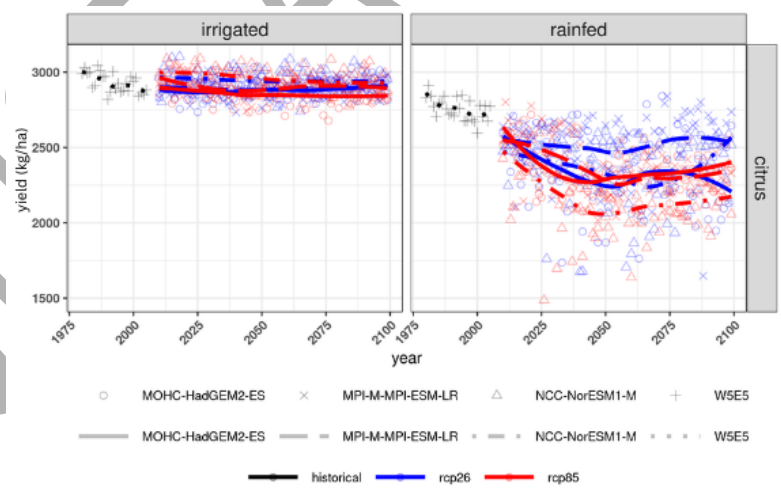

Figure 5. National level yield trends (kg/ha) for citrus trees under irrigated and rainfed conditions for RCPs 2.6 and 8.5 over the 2010-2099 period. Future yield simulations were based on three GCMs and historical information on the W5E5 dataset.

3.3. Attributing adverse weather conditions to changes in crop yields

On average, weather extremes explained 28% and 33% of the yield variability over time under RCPs 2.6 and 8.5, respectively (Fig. 6). The impacts were also crop-dependent, with a high level of uncertainty between crops, ranging from high (rice) to low (citrus and wheat). The crops most affected by adverse weather conditions were citrus and common beans under RCPs 2.6 and 8.5, respectively. Furthermore, the most impactful adverse weather condition, explaining 20% to 50% of the yield changes for all ten crops, was heat stress, followed by dry spells (Fig. 7). Nonetheless, the impact of dry spells on yields increased with higher model sensitivity to GHGs, showing an opposite trend to that of heat stress. The latter was highlighted by the transparency of the colors (e.g., high transparency in Fig. 7 corresponded to a low R^2 value).

The following analysis focuses on those crops most likely to be affected by different abiotic stresses (Fig. 8). The number of consecutive dry days will increasingly affect crop yields under RCP 8.5 compared to RCP 2.6. Although wet days (here defined as heavy rainfall events with a dynamic threshold selected based on statistical significance) affected a small number of crops, their impact was higher under RCP 8.5. Overall, the findings suggested that erratic rainfall (e.g., heavy rainfall events followed by dry periods) will increasingly affect crop yields under RCP 8.5. Thus, under RCP 8.5, precipitation will be the main limiting factor reducing crop yields, exceeding the effect of heat stress, which was the most impactful weather hazard under RCP 2.6

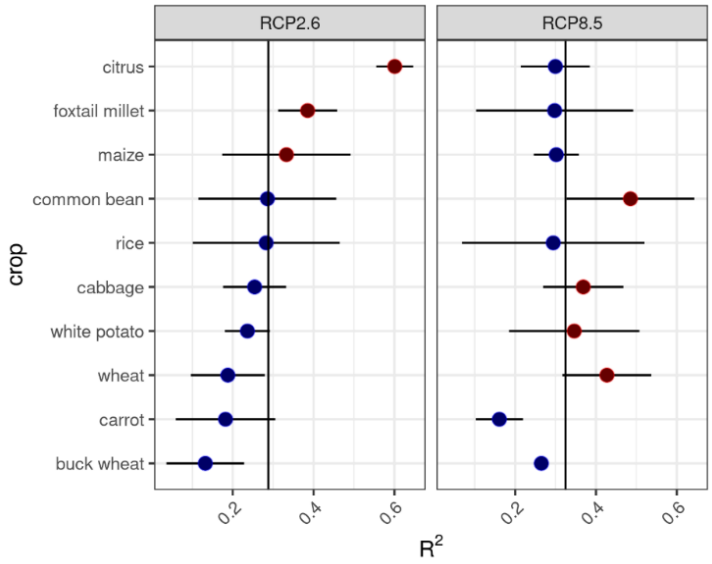

Figure 6. Impact of weather extremes on crops and associated uncertainty between GCMs.

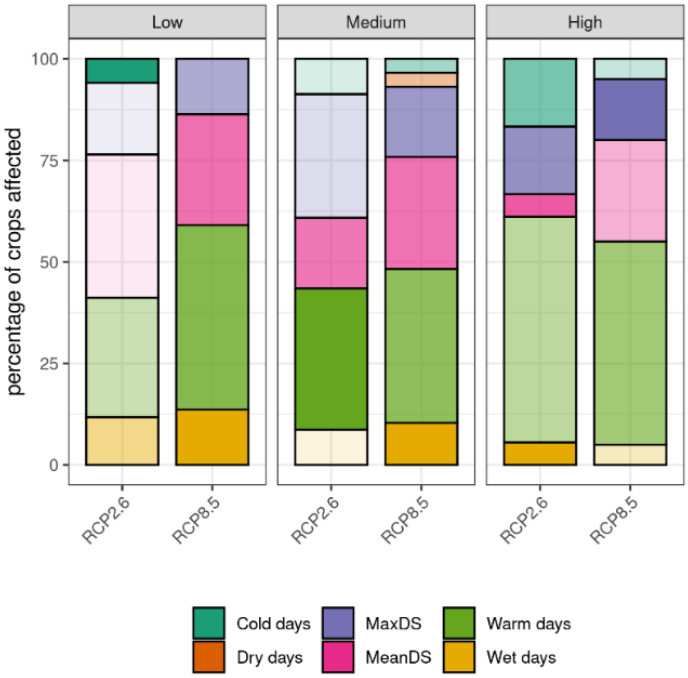

Figure 7. Percentage of crops affected by weather extremes based on different RCPs and GCMs sensitivity to GHG emissions (high: HadGEM2-ES; medium: MPI-ESM; low: NorESM1-M). The high transparency of the color indicated a low R^2 value.

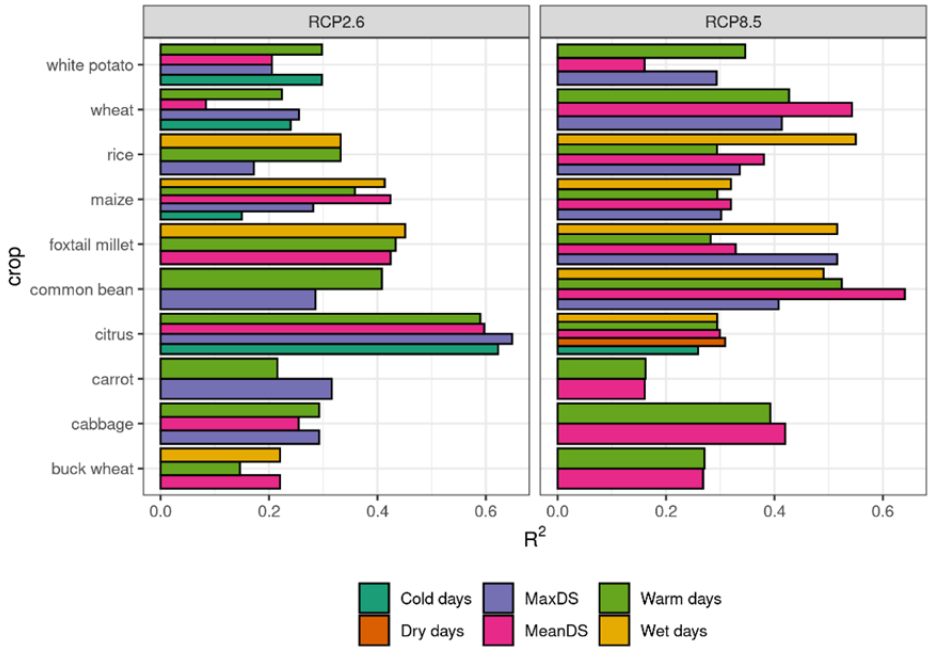

Figure 8. Impact of weather extremes on targeted crops for the ensemble of GCMs.

4. Discussion

396 This work described the relationship between weather extremes and crop yields, explaining about 28% and
397 33% of the yield variation over time under RCPs 2.6 and 8.5, respectively. Heat stress and dry spells were
398 identified as the most impactful weather hazards, accounting for 20% to 50% of the yield anomalies across
399 the century. Thus far, no national-level impact assessments have examined the effect of elevated heat stress
400 on crop production in Bhutan. However, regional studies have shown that yield gains due to the CO_2
401 fertilization effect would be offset by the negative impact of a 2ºC increase in mean daily surface
402 temperatures on irrigated rice and rainfed wheat (Lal, 2011). Studies also indicated a more significant
403 warming during the spring and winter seasons, leading to shifting growing seasons, accelerated crop
404 growth, increased evapotranspiration rates, affected pollination dynamics, and elevated pressure from pests
405 and diseases on crops (e.g., wheat and maize).
406
407 Regarding precipitation indices, past climate analyses point to an increasing trend in the number of
408 consecutive dry days during the 1996-2001 period across Bhutan (Llamo et al. 2023). While scientific
409 studies are available on seasonal precipitation trends, little is known about precipitation extremes in Bhutan.
410 Projections indicate an increase in total annual rainfall ranging from +10% to +30% under RCP 4.5 by
411 2070-2099, with a +5% to +15% increase in summer rainfall (NEC, 2020). The latter results align with this
412 study's findings on total annual precipitation, though depending on the RCP (annual results not shown for
413 brevity). However, conflicting findings emerged for monthly precipitation. While our findings pointed to a
414 widespread loss in August and September, particularly under RCP 8.5, NEC (2020) suggested an increase.
415 The compounded effect of weather perils, together with a slight increase (0 to +2 days for both RCPs) in
416 the number of days with heavy precipitation ($R \geq 20$ mm/day) on an annual average (results not shown for
417 brevity), are expected to have severe consequences (e.g., uprooting crops and waterlogging soils) on some
418 of the studied crops, particularly among shallow-rooted (e.g., vegetables) and high-water-demanding crops
419 (e.g., rice and maize).
420
421 Existing literature (e.g., NEC, 2011, 2020) on future crop yields in Bhutan, using the Decision Support
422 System for Agrotechnology Transfer (DSSAT) model and the A1B Special Report on Emission Scenarios
423 (SRES), showed a mean yield change for maize (without the CO_2 fertilization effect) ranging from -21%
424 to -7% by 2040-2069. Conversely, our findings suggested stable yield trends under RCP 2.6 and a slight

425 decline (-2.1%) under RCP 8.5. Although there is a likelihood of a decline in maize suitability areas, the
426 reported loss is not significant (-3.4%) under RCP 4.5 by 2070 (NEC, 2020). The decline in maize yields
427 was attributed to water deficits and accelerated crop development, which resulted in lower biomass
428 accumulation and, consequently, in a yield decline. Similarly, in Nepal, a 20-day reduction in the growing
429 cycle of maize was expected under RCPs 4.5 and 8.5 by the end of the century across the mid-hills (Alvar-
430 Beltrán et al. 2023). Furthermore, Parker et al. (2017) study, using the EcoCrop database of crop constraints
431 and characteristics together with an ensemble of 31 GCMs, showed an increasing precipitation pattern
432 across Bhutan. As a result, the suitability areas for maize were likely to increase in the future compared to
433 the baseline period, particularly under RCP 8.5 and in the high-altitude areas of eastern Bhutan. However,
434 a decline in maize yields was detected towards the southeastern parts due to critical temperatures exceeding
435 the threshold for maize pollination.
436
437 For rice, a crop with a C3 photosynthetic pathway, the uncertainties were much higher with and without
438 the CO_2 fertilization effect. Our results, which did not account for the CO_2 fertilization effect, showed an
439 average (ensemble of GCMs for both rainfed and irrigated conditions) yield loss of -1% under RCP 8.5 by
440 the end of the century. In contrast, NEC (2011) projected a yield change ranging from +72% to -27% by
441 2040-2069 depending on the climate scenario. Rice suitability may increase in the dzongkhag of Punakha,
442 as well as in the eastern and southeastern parts of the country under RCPs 4.5 and 8.5, driven by optimal
443 growing conditions and the CO_2 fertilization effect (Parker et al. 2017). Generally, an increase ranging from
444 +8.9% to +13.9% in rice suitability areas was projected under RCPs 4.5 and 8.5 by 2050, with a decline (-
445 3.3%) under RCP 8.5 by 2070 (NEC, 2020).
446
447 Similar to rice, wheat production under rainfed conditions might experience a yield gain (+15.5% for RCP
448 8.5 by the end of the century) in Bhutan, partially because future temperatures are not expected to exceed
449 the critical threshold (Tmax >32ºC) for pollen viability, as reported across different agroclimatic zones of
450 Nepal (Alvar-Beltrán et al. 2023). However, the combined effect of elevated CO_2 and heat stress during
451 meiosis can reduce pollen viability, spikelet number, and grain yield per spike (Bokshi et al. 2021).
452 Additionally, NEC (2011) projected a positive yield trend for potatoes (+19% to +89% depending on the
453 GCM) in Phobjikha, aligning with this study's findings (+17.7%) under rainfed conditions for RCP 8.5.

Parker et al. (2017) also suggested that lower altitude areas in the south (<1000 m.a.s.l.) will not be longer be suitable for potato production due to increasing temperatures, while mid- and high-altitude areas (1000-3000 m.a.s.l.) may experience an expansion in crop suitability over time, particularly under RCP 8.5 by 2050.

Although there is no scientific evidence on future climate impacts on vegetables, legumes, and tree crops in Bhutan, 10% to 20% damages in crop production (e.g., vegetables, mandarins, and apples) were already reported by the DoA between 2014 and 2016 (Chhogyel et al. 2020). Our work revealed an increase in the exposure of vegetables to weather adversities, particularly of cabbage, which is increasingly exposed and, thus, affected by a higher number of warm days and prolonged dry spells under RCP 8.5. However, citrus trees are expected to be less exposed to cold days under RCP 8.5. Under a warmer climate, citrus trees could expand to higher altitude areas (up to 1500 m.a.s.l.) in Nepal, which have similar bioclimatic characteristics to those of Bhutan (Atreya and Kaphle, 2020). However, higher temperatures and evaporation rates during flowering and fruit set could result in detrimental effects to citrus production in Bhutan.

5. Conclusions

Climate impact potential assessments in crop production are at an early stage in Bhutan. Although climate and crop and eco-physiological models and datasets can contain limitations (e.g., the quality and reliability of some of the underlying datasets of PyAEZ are known to be uneven across regions and the CO_2 fertilization effect is not considered in PyAEZ), if adequately processed, through statistical means and their weaknesses well understood, they can be valuable for attributing adverse weather conditions to agricultural production and to assist field management decision-making in both rainfed and irrigated agriculture in Bhutan. The latter attribution allowed us to discern the weather hazards likely to be most harmful (i.e., heat stress and dry spells) to specific crops and, thus, to guide climate actions on the ground. The emerging findings of this work (see summary Table 2) can also be advantageous to identify tailored adaptation solutions, including the selection of most suitable sowing dates based on future climatic conditions, water allocation and water-related policies, which can modulate, to a certain extent, future weather perils on studied crops.

This study also showed the irrigation potential to increase yields by +43.4% on average for all crops and RCPs across the century. In this line, adequate planning and implementation of irrigation systems recognizing the detrimental effects of climate change need to be thoroughly considered in water resource inventories aiming to strengthen the existing National Integrated Water Resource Management Plan. Agro-biodiversity is often cited in literature as one of the potential solutions to adapt to climate change in Bhutan, mainly through the development and use of biotic and abiotic tolerant varieties, strengthening the traditional seed system, and enhancing the on-farm diversity as an insurance to climate change impacts.

Overall, our findings not only represent an opportunity for future crop-specific modelling work assessing the most effective agricultural adaptation solutions in Bhutan but are also a novel source of information for climate risk assessments in agriculture across Bhutan. Beyond providing a snapshot of climate change impacts on agriculture production in Bhutan, the emerging findings of this study are a steppingstone to facilitate the work of project formulators, development agencies, agricultural extension, and decision-makers, among others, when developing projects, policies and strategies based on factual information that relies on the best available climate information (CORDEX-CORE) for impact assessment studies in agriculture.

Table 2. Summary of yield changes (%) for selected crops under rainfed and irrigated conditions for 2070-2099 (average of all 3 GCMs) compared to 2010-2039 for RCPs 2.6 and 8.6.

	Rainfed		Irrigated		% differences
Grain maize	RCP 2.6	RCP 8.5	RCP 2.6	RCP 8.5	(irrigated and rainfed)
Grain maize	-1.9	-5.8	+0.3	-1.3	+24
Foxtail millet	+0.3	-2.1	+0.7	+0.3	+25
Buckwheat	+1.4	-3.4	+0.7	+0.2	+62
Wheat (subtropical cultivar)	+0.1	-6.7	+0.5	=	+46
Wetland rice	-1.0	+15.3	+0.7	+5.4	+62
Common beans	+0.2	-1.6	+0.4	-0.4	+42
Cabbage	=	-4.8	+0.7	-0.4	+26
White potatoes	-0.3	+12.8	+1.0	+4.7	+53
Carrots	-0.6	+17.4	+0.8	+5.5	+72
Citrus	+0.1	-3.9	+0.6	+1.0	+22

Differences between irrigated and rainfed conditions are performed for the ensemble of GCMs and RCPs across the century.

Acknowledgements

The analysis was initiated under the implementation of a World Bank project "Bhutan: Climate Impacts in Bhutan's Agroecological Zones and Opportunities for Climate-Smart Agriculture Practices". The authors recognize the invaluable support provided by the World Bank (Christine Heumesser) and FAO (Riccardo Soldan) technical experts during the conceptualization of this analytical work.

References

Allen, R.G., Pereira, L.S., Raes, D. and Smith, M., 1998. Crop Evapotranspiration (guidelines for computing crop water requirements), Drainage and Irrigation Paper N 56. Rome, Italy, Food and Agriculture Organization of the United Nations.

Alvar-Beltrán, J., Soldan, R., Vanuytrecht, E., Heureux, A., Shrestha, N., Manzanas, R., Pant, K.P. and Franceschini, G., 2023. An FAO model comparison: Python Agroecological Zoning (PyAEZ) and AquaCrop to assess climate change impacts on crop yields in Nepal. *Environmental Development*, *47*, p.100882.

Atreya, P.N. and Kaphle, M., 2020. Visible evidence of climate change and its impact on fruit production in Nepal. International Journal of Agriculture Environment and Food Sciences, 4(2), pp.200-208.

Beck, C., Grieser, J., Kottek, M., Rubel, F., and Rudolf, B. 2005. Characterizing global climate change by means of Köppen climate classification. Klimastatusbericht, 51, 139-149.

Bokshi, A.I., Tan, D.K., Thistlethwaite, R.J., Trethowan, R. and Kunz, K., 2021. Impact of elevated CO2 and heat stress on wheat pollen viability and grain production. *Functional Plant Biology*, *48*(5), pp.503-514.

Chhogyel, N., Kumar, L., Bajgai, Y., and Hasan, M. K. 2020. Perception of farmers on climate change and its impacts on agriculture across various altitudinal zones of Bhutan Himalayas. International Journal of Environmental Science and Technology, 17(8), 3607-3620.

Chhogyel, N., and Kumar, L. 2018. Climate change and potential impacts on agriculture in Bhutan: a discussion of pertinent issues. Agriculture & food security, 7(1), 1-13.

Choden, K., Keenan, R. J., and Nitschke, C. R. 2020. An approach for assessing adaptive capacity to climate change in resource dependent communities in the Nikachu watershed, Bhutan. Ecological Indicators, 114, 106293.

Coppola, E., Raffaele, F., Giorgi, F., Giuliani, G., Xuejie, G., Ciarlo, J.M., Sines, T.R., Torres-Alavez, J.A., Das, S., di Sante, F. and Pichelli, E., 2021. Climate hazard indices projections based on CORDEX-CORE, CMIP5 and CMIP6 ensemble. Climate Dynamics, 57, pp.1293-1383.

Cucchi, M., Weedon, G. P., Amici, A., Bellouin, N., Lange, S., Müller Schmied, H., & Buontempo, C. 2020. WFDE5: bias-adjusted ERA5 reanalysis data for impact studies. Earth System Science Data, 12(3), 2097-2120.

Department of Agriculture (DoA). 2016. Agriculture statistics 2015. Thimphu. Ministry of Agriculture and Forests (MoAF), Royal Government of Bhutan.

Fischer, G., Nachtergaele, F.O., van Velthuizen, H.T., Chiozza, F., Franceschini, G., Henry, M., Muchoney, D. and Tramberend, S. 2021. Global Agro-Ecological Zones v4 – Model documentation. Rome, FAO.

Food and Agriculture Organization (FAO). 2017. National Agro-Economic Zoning for Major Crops in Thailand (NAEZ). Available online at: link

Giorgi, F., Coppola, E., Jacob, D., Teichmann, C., Abba Omar, S., Ashfaq, M., Ban, N., Bülow, K., Bukovsky, M., Buntemeyer, L. and Cavazos, T., 2021. The CORDEX-CORE EXP-I initiative: description and highlight results from the initial analysis. Bulletin of the American Meteorological Society, pp.1-52.

International Labour Organization (ILO). 2019. Data, resources: statistics on employment. Available online at: link

Kassam, A. H., Van Velthuizen, H. T., Fischer, G. W., and Shah, M. M. 1991. Agro-ecological land resources assessment for agricultural development planning. A case study of Kenya. Resources data base and land productivity. Technical Annex, 1, 9-31.

Kassam, A. H. 1977. Net Biomass Production and Yield of Crops with Provisional Results for Tropical Africa. Soil Resources, Management and Conservation Service, Land and Water Development Division, FAO.

Katwal, T.B., Dorji, S., Dorji, R., Tshering, L., Ghimiray, M., Chhetri, G.B., Dorji, T.Y. and Tamang, A.M., 2015. Community perspectives on the on-farm diversity of six major cereals and climate change in Bhutan. *Agriculture*, *5*(1), pp.2-16.

Lal, M., 2011. Implications of climate change in sustained agricultural productivity in South Asia. *Regional Environmental Change*, *11*(Suppl 1), pp.79-94.

Latham, J., Cumani, R., Rosati, I. & Bloise, M., 2014. Global Land Cover SHARE (GLC-Share) database Beta-Release Version 1.0. Rome, Italy, FAO of the United Nations. 40 pp. Available online at: link

Lhamo, T., Chen, G., Dorji, S., Tamang, T.B., Wang, X. and Zhang, P., 2023. Trends in Extreme Precipitation Indices over Bhutan. *Atmosphere*, *14*(7), p.1154.

Ministry of Agriculture and Forests (MoAF). 2011. National action plan biodiversity persistence and climate change. Timphy: MoAF, Royal Government of Bhutan. Available online at: link

Nachtergaele, F.O., van Velthuizen, H., Verelst, L. & Wiberg, D. 2012. Harmonized World Soil Database (version 1.2). Rome, Italy, FAO, International Institute for Applied Systems Analysis (IIASA), ISRIC-World Soil Information, Institute of Soil Science – Chinese Academy of Sciences (ISSCAS), Joint Research Centre of the Europe. 50 pp. Available online at: link

National Environmental Commission (NEC). 2023. National Adaptation Plan (NAP) of the Kingdom of Bhutan. Available online at: link

National Environmental Commission (NEC). 2020. Third National Communication to the UNFCCC, 2020. Available online at: link

National Environmental Commission (NEC). 2016. Water in Bhutan's economy: importance to partners. Available online at: link

National Environmental Commission (NEC). 2011. Second National Communication from Bhutan to the UNFCCC. Available online at: link

Naveendrakumar, G., Vithanage, M., Kwon, H.H., Chandrasekara, S.S.K., Iqbal, M.C.M., Pathmarajah, S., Fernando, W.C.D.K. and Obeysekera, J., 2019. South Asian perspective on temperature and rainfall extremes: A review. Atmospheric Research, 225, pp.110-120.

Parker, L., Guerten, N., Nguyen, T. T., Rinzin, C., Tashi, D., Wangchuk, D., and Penjor, S. 2017. Climate change impacts in Bhutan: challenges and opportunities for the agricultural sector. *CCAFS Working Paper*.

Teichmann, C., Jacob, D., Remedio, A.R., Remke, T., Buntemeyer, L., Hoffmann, P., Kriegsmann, A., Lierhammer, L., Bülow, K., Weber, T. and Sieck, K., 2021. Assessing mean climate change signals in the global CORDEX-CORE ensemble. Climate Dynamics, 57, pp.1269-1292.

SUPPLEMENTARY FIGURES

A **B**

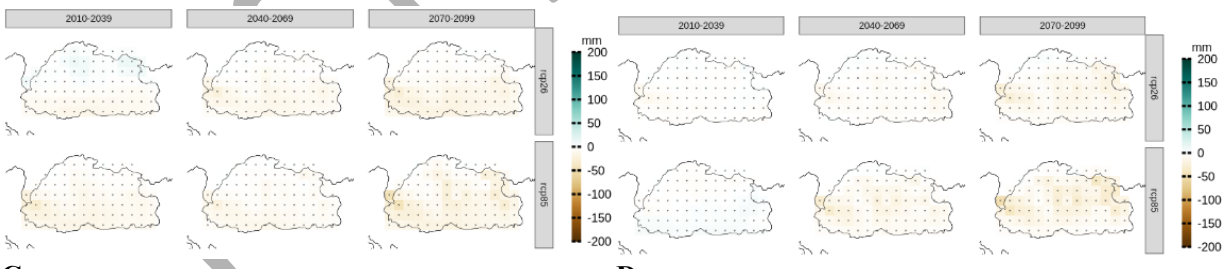

C **D**

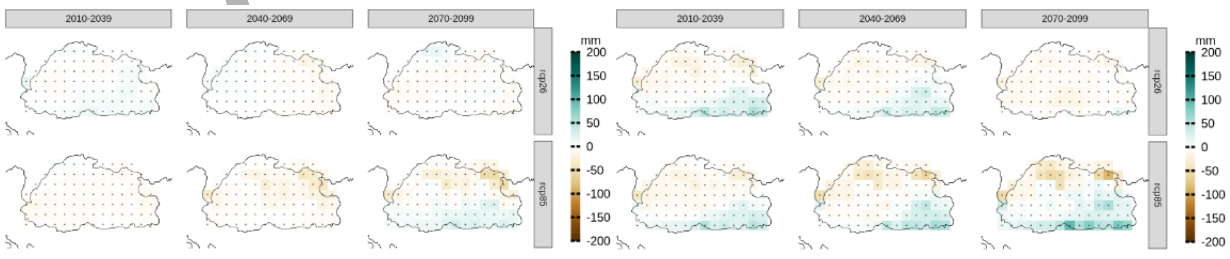

E **F**

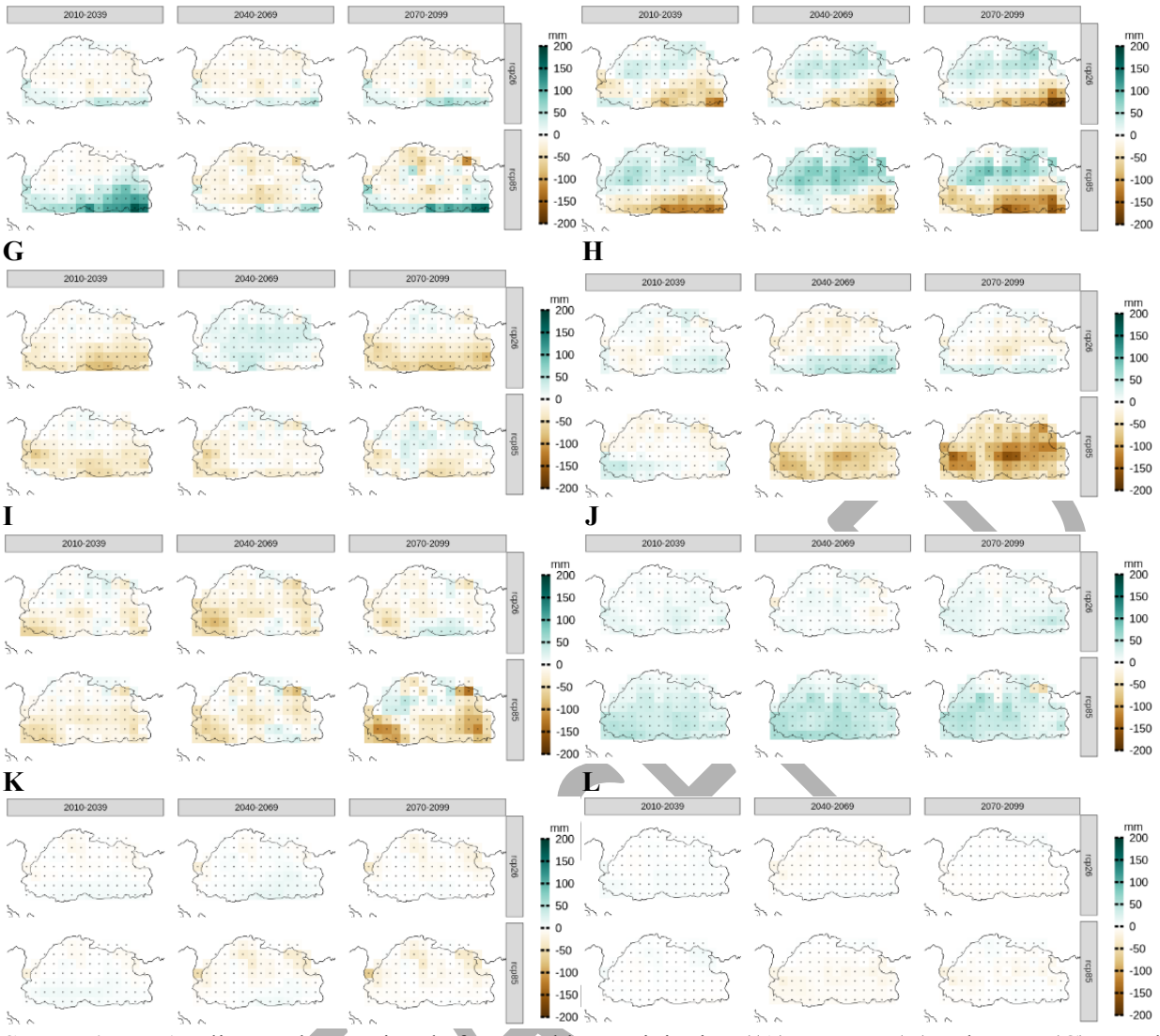

Supp. Figure 1. Climate change signals for monthly precipitation ((**A**) January, (**B**) February, (**C**) March, (**D**) April, (**E**) May, (**F**) June, (**G**) July, (**H**) August, (**I**) September, (**J**) October, (**K**) November, and (**L**) December) for the different time-periods (2010-2039; 2040-2069; 2070-2099) and RCPs (2.6 and 8.5).

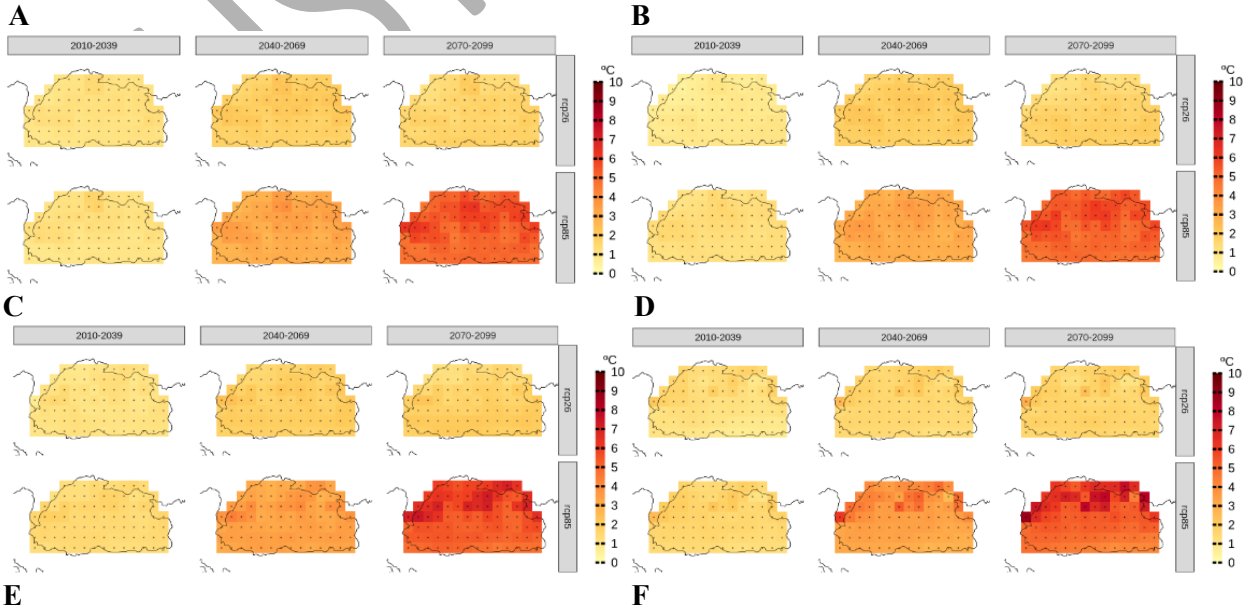

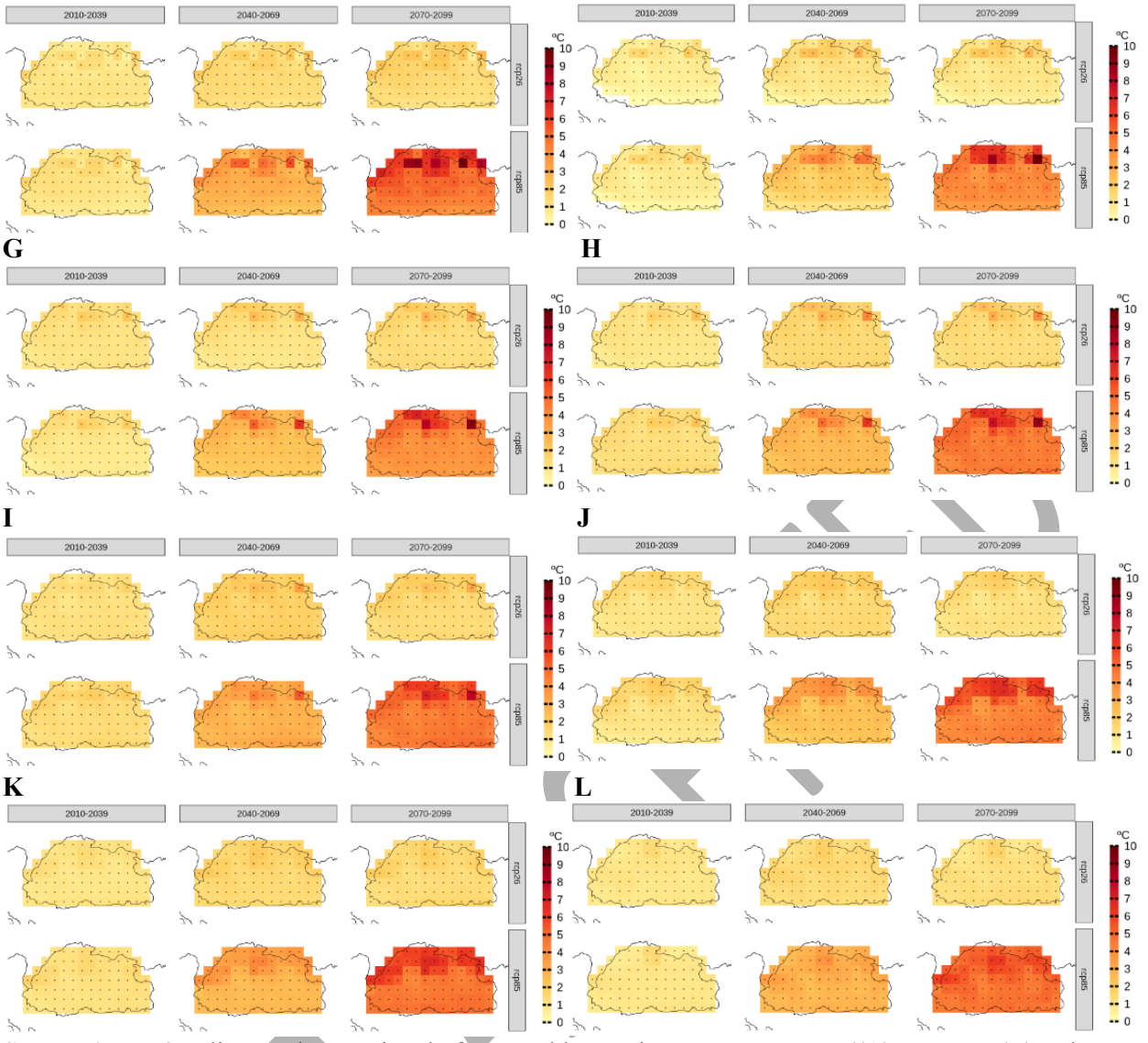

Supp. Figure 2. Climate change signals for monthly maximum temperature ((**A**) January, (**B**) February, (**C**) March, (**D**) April, (**E**) May, (**F**) June, (**G**) July, (**H**) August, (**I**) September, (**J**) October, (**K**) November, and (**L**) December) for the different time-periods (2010-2039; 2040-2069; 2070-2099) and RCPs (2.6 and 8.5).

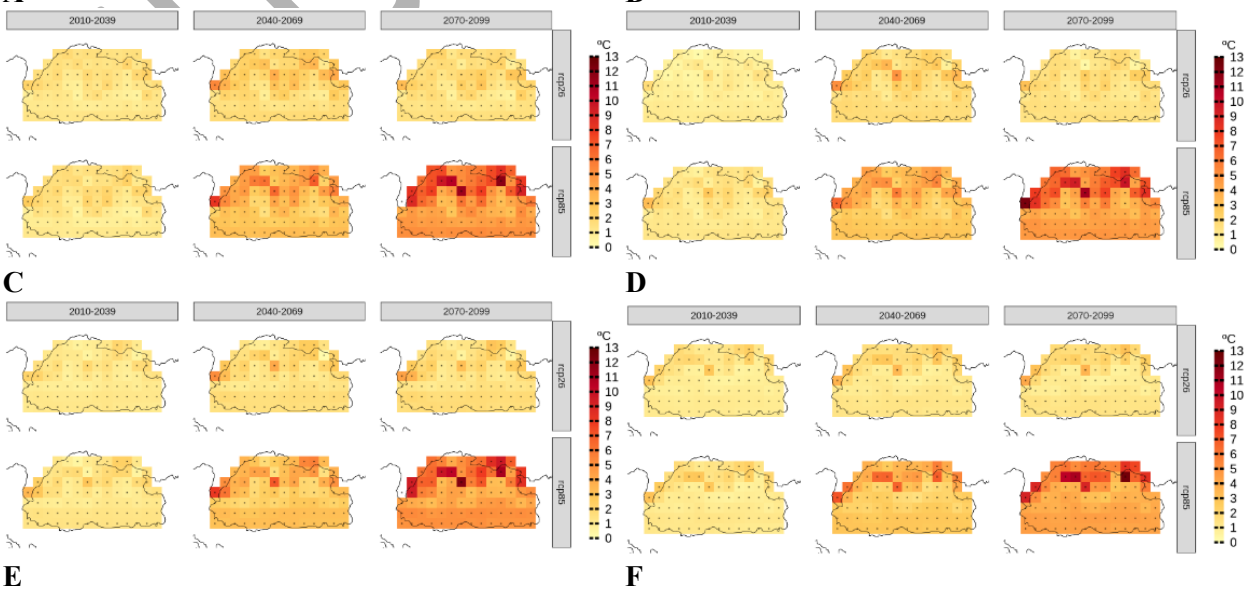

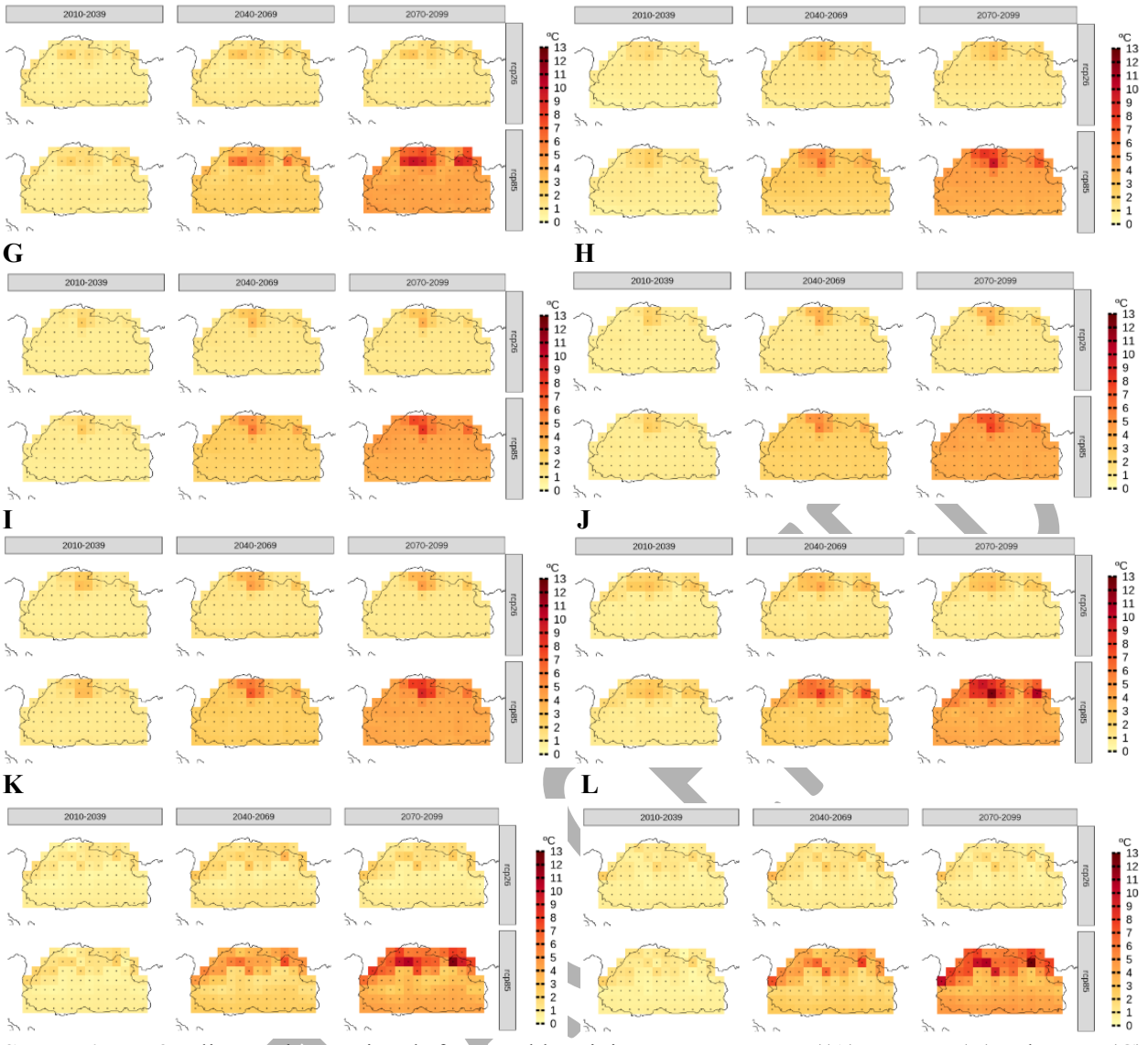

Supp. Figure 3. Climate change signals for monthly minimum temperature ((**A**) January, (**B**) February, (**C**) March, (**D**) April, (**E**) May, (**F**) June, (**G**) July, (**H**) August, (**I**) September, (**J**) October, (**K**) November, and (**L**) December) for the different time-periods (2010-2039; 2040-2069; 2070-2099) and RCPs (2.6 and 8.5).

a) Grain maize

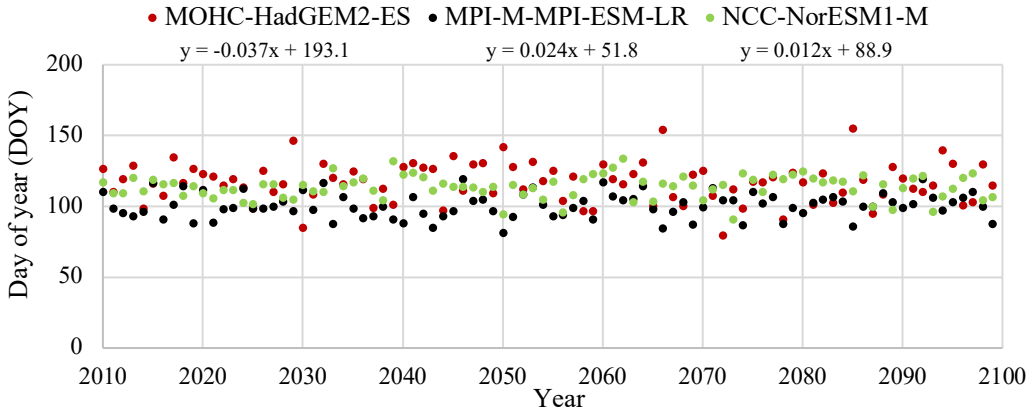

b) Foxtail millet

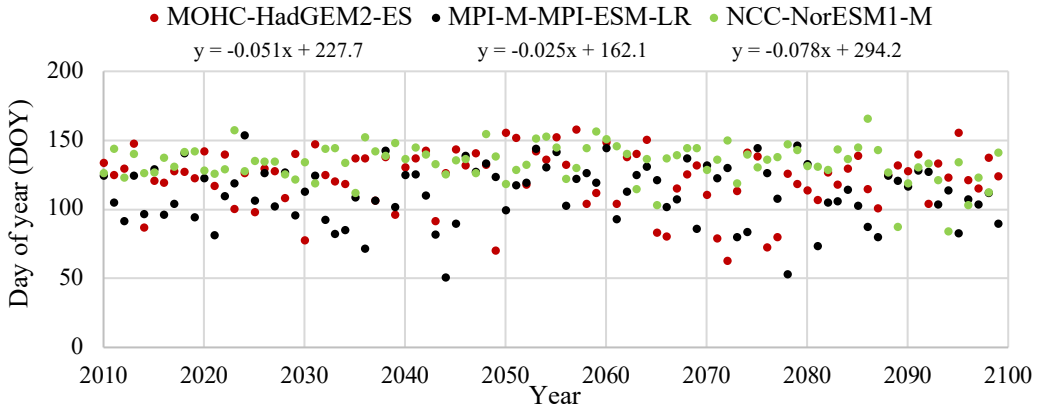

c) Buckwheat

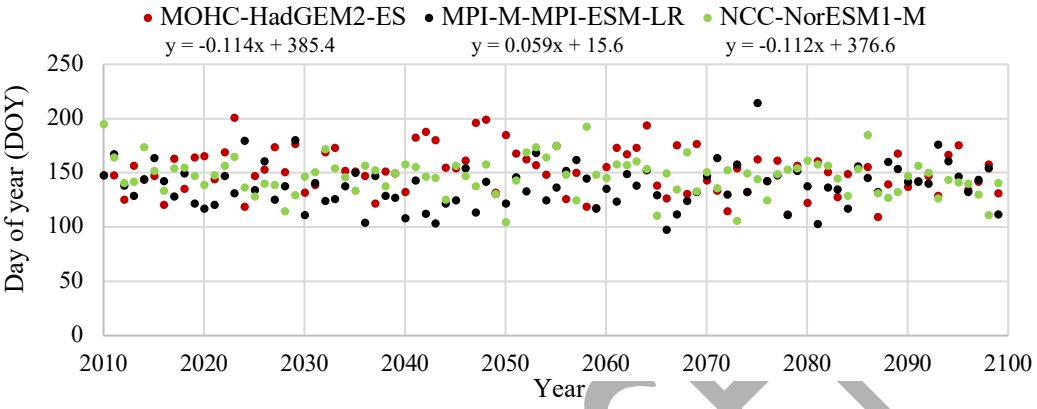

d) Wheat

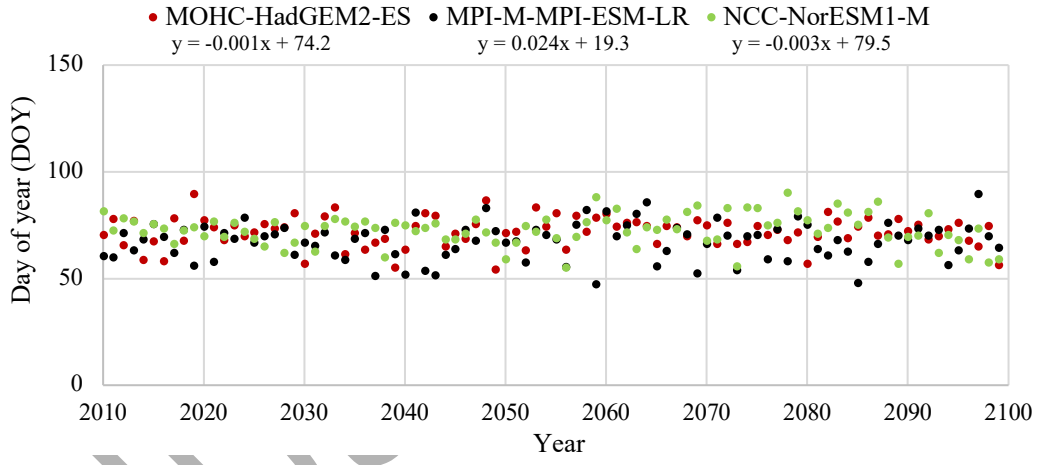

e) Wetland rice

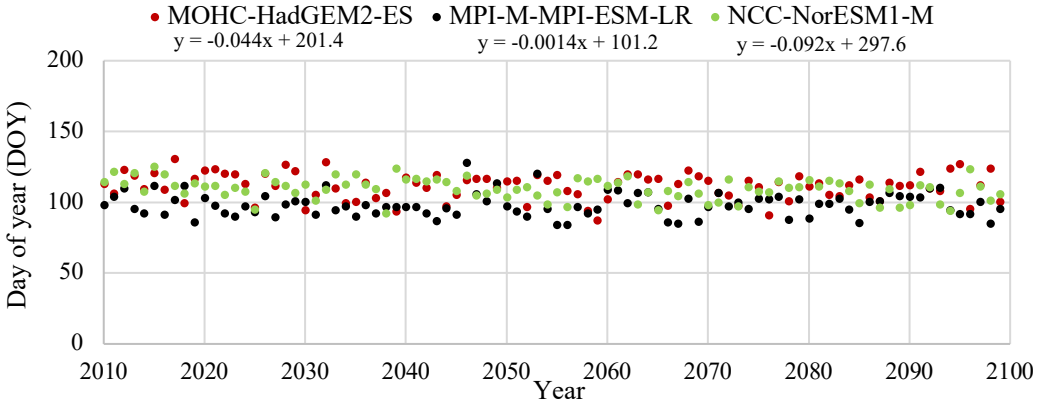

f) Common beans

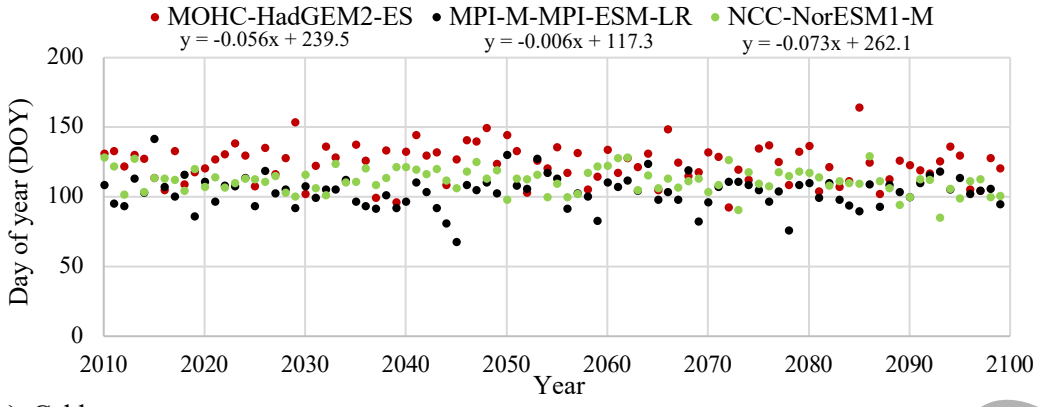

g) Cabbage

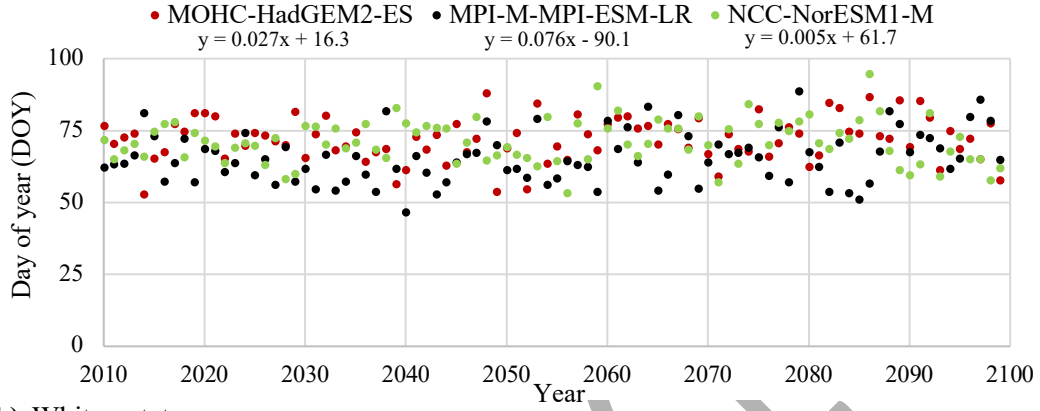

h) White potatoes

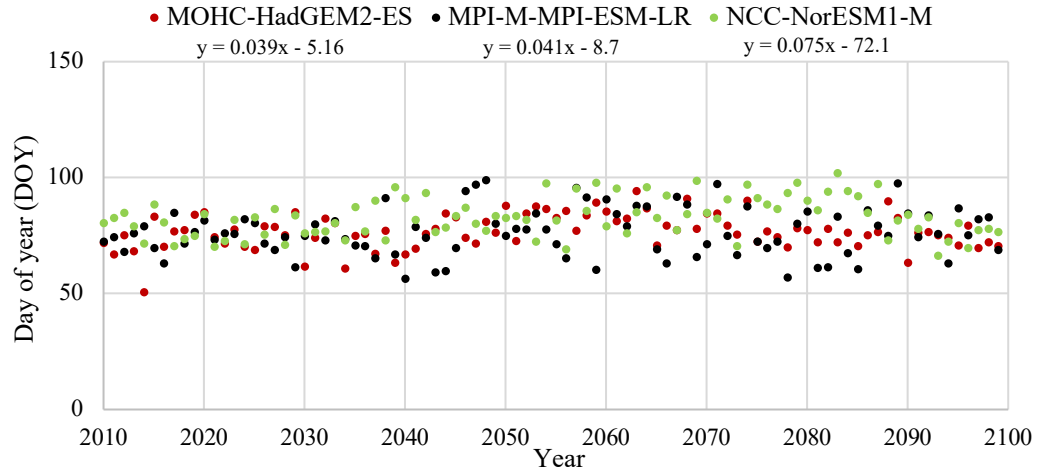

i) Carrots

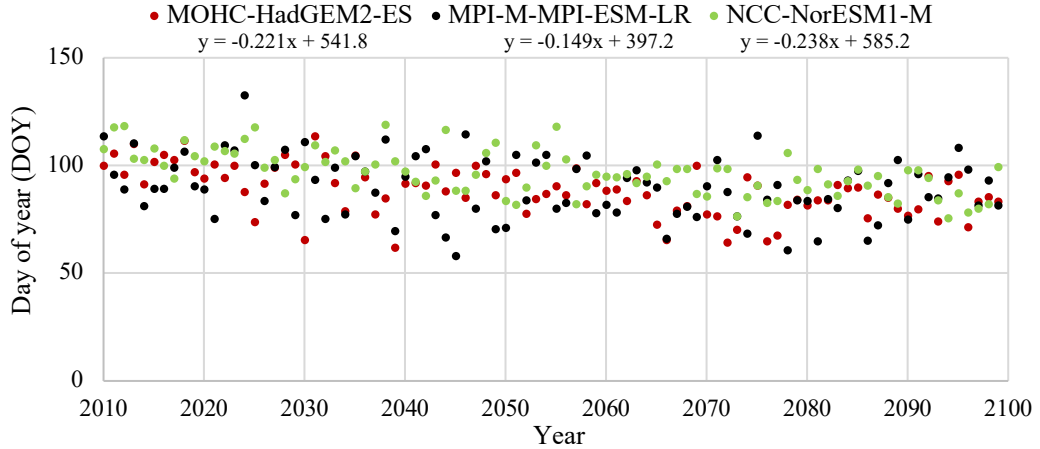

733 **Supp. Figure 4.** Starting date of crop growth (day of the year) and regression line for all GCMs based on
734 PyAEZ simulations.
735
736 *Note: results for citrus trees were not considered in the analysis of Supp. Fig.4.*